Biosensors and Bioelectronics 47 (2013) 402–407

Contents lists available at SciVerse ScienceDirect

Biosensors and Bioelectronics

journal homepage: www.elsevier.com/locate/bios

A simple and sensitive fluorescence biosensor for detection of organophosphorus pesticides using H_2O_2-sensitive quantum dots/bi-enzyme

Xianwei Meng [a], Jianfei Wei [a,b], Xiangling Ren [a], Jun Ren [a,*], Fangqiong Tang [a,*]

[a] Laboratory of Controllable Preparation and Application of Nanomaterials, Technical Institute of Physics and Chemistry, Chinese Academy of Sciences, No. 29, Zhongguancun East Road, Haidian District, Beijing 100190, People's Republic of China
[b] University of Chinese Academy of Sciences, Beijing 100049, People's Republic of China

ARTICLE INFO

Article history:
Received 18 November 2012
Received in revised form
16 March 2013
Accepted 19 March 2013
Available online 2 April 2013

Keywords:
Quantum dots
Dichlorvos
Enzyme biosensor
Inhibition
Real sample
Simple

ABSTRACT

In this paper, we have developed a simple, fast, convenient and sensitive method for determination of organophosphorus pesticides in real samples based on inhibition mechanism of acetylcholinesterase (AChE). The biosensor is composed of enzymes (AChE and ChOx (choline oxidase)), QDs and acetylcholine (ACh), without any complex process of assembly for biosensor. After the experimental conditions are optimized, the limit of detection (LOD) for dichlorvos (DDVP) is found to be 4.49 nM. Two linear ranges allow a wide determination of DDVP concentration from 4.49 nM to 6780 nM. Furthermore, a possible mechanism is put forward to explain the fluorescence quenching of CdTe QDs in the presence of H_2O_2. More importantly, the obtained biosensor is proven to be suitable for the detection of residues of organophosphorus pesticides (OPs) in real examples. The excellent performance of this biosensor will facilitate future development of rapid and high-throughput detection of organophosphorus pesticides.

1. Introduction

The pesticide is an important management tool to boost agricultural productivity—increase crop yield and reduce post-harvest losses, especially in a world facing a hunger crisis and famine. Due to high efficiency for insect elimination, easy synthesis, and low cost, organophosphorous pesticides are the subclass of pesticides most widely used in agriculture (Masumoto and Sonobe, 1997). According to Pesticide Action Network North America, about 70% of the insecticides in current use are OPs in the United States. As a result of the widespread use of OPs, their residues can be frequently found in fruits and vegetables. Unfortunately, the residues of OPs could cause serious health problem for human even at very low concentrations. OPs can induce acute and chronic neurotoxicity in mammals primarily by inhibiting AChE (Sarabia et al., 2009; Shenouda et al., 2009), which is important in helping regulate nerve impulses. After OPs irreversibly react with AChE, the subsequent accumulation of ACh in the cholinergic clefts causes overstimulation of the peripheral as well as the central cholinergic nervous system (Yadav et al., 2012). The symptoms of organophosphorous poisoning include headache, dizziness, salivation, lacrimation, sweating, vomiting, diarrhea, abrupt tremor, lung edema, coma and even death from respiratory or cardiac failure. Besides these neurotoxic effects, the oncogenic and teratogenic risk caused by OPs is another concern (Curl et al., 2002). To eliminate the abuse of OPs and protect the health of the public, it is of important significance to develop a simple and sensitive method for the on-site and real-time detection of OPs residue.

Various conventional instrument-based methods have been adopted for the detection of OPs, in which chromatographic techniques are the most accurate quantitative analysis method for the assessment of OP compounds in real samples. However, the chromatographic equipment is bulky and expensive, and sample pretreatment process is rather complicated and strict. The whole analysis process has to be performed by highly qualified technicians. As a result, they are not suitable for prompt on-site and real-time detection. In order to circumvent these problems, scores of OPs biosensors have been proposed based on the inhibition mechanism of AChE and different transduction technologies (electrochemistry, fluorescence, colorimetric probes etc.) (Andreescu and Marty, 2006; Constantine et al., 2003; Dondoi et al., 2006; Hossain et al., 2009; Karnati et al., 2007; Sotiropoulou et al., 2005; Su et al., 2008; Suwansa-ard et al., 2005; Vamvakaki and Chaniotakis, 2007). Due to the exceptional photophysical properties, QDs are gaining interest as fluorescent probe. Based on the fluorescence switch of QDs, Liu and coworkers prepared a

* Corresponding author. Tel.: +86 10 82543521; fax: +86 10 62554670.
E-mail address: tangfq@mail.ipc.ac.cn (F. Tang).

0956-5663/$ - see front matter © 2013 Elsevier B.V. All rights reserved.
http://dx.doi.org/10.1016/j.bios.2013.03.053

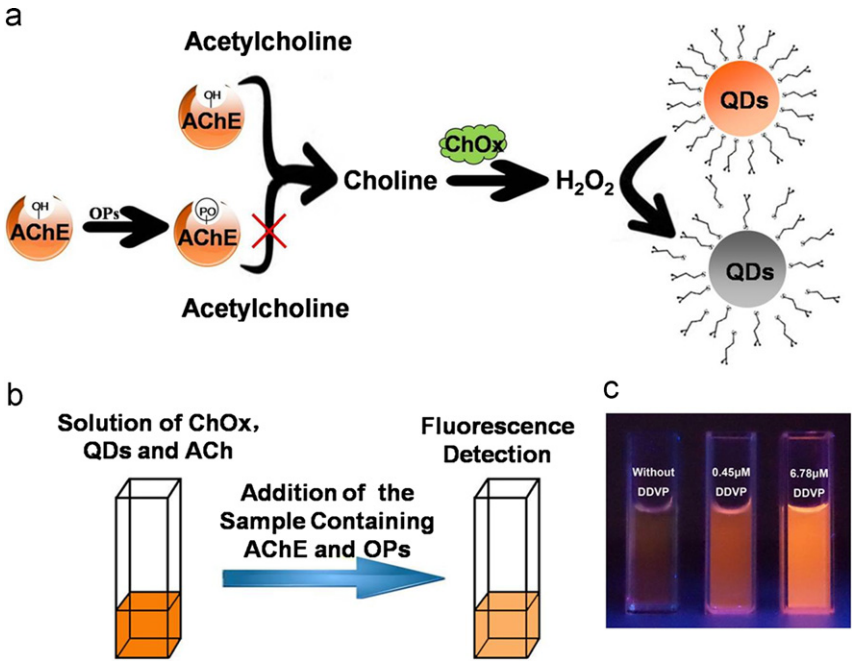

Scheme 1. (a) Schematic principle for the detection of OPs; (b) the process for the detection of OPs; (c) the color change with different concentrations of DDVP (0 μM, 0.45 μM and 6.78 μM) in the detection process .

biosensor for the detection of OPs in real fruit and vegetable samples, which was fabricated using the layer-by-layer (LBL) assembly technique (Zheng et al., 2011a). Unfortunately, the tens layers of films assembled by the LBL technique are associated with some disadvantages, such as low efficiency, time-consuming and tedious processing steps for preparing biosensors. Hence, there is an increasing need to develop simple and sensitive methods for detecting the residues of OPs in daily-consumed foods and drinking water.

In this paper, we developed a simple, rapid, and sensitive method for optical detection of organophosphorus pesticides, which is based on inhibition mechanism of AChE (Scheme 1(a)). This method only composes one step in the detection of OPs, blending the sample with AChE and the solution containing ACh, ChO*x* and QDs (Scheme 1(b)), without complex process of assembly for biosensor. We choose DDVP as an example of organophosphorus pesticides, because DDVP has been widely used throughout the world in agriculture for controlling insects that damage crops (Yadav et al., 2012), especially in developing nations (Sunkaria et al., 2012). The results exhibited a good linear relationship in the range of 4.49–896 nM and 2240–6780 nM. The obtained biosensor showed low detection limit (4.49 nM). Furthermore, we proposed a possible mechanism of the fluorescence quenching of CdTe QDs in the presence of H_2O_2. At the initial stage of the quenching of QDs, the reason for the quenching was mainly the detaching of thiolation from the surface of QDs. When the QDs were seriously quenched, the quenching of QDs was due to the combination of the detaching of thiolation from the surface of QDs and the oxidation of Te. Our results also reveal that the proposed biosensor can be applied in real samples.

2. Experimental

2.1. Materials

AChE (EC 3.1.1.7, from Electrophorus electricus (electric eel.), 425.94 Units/mg), ChO*x* (EC 1.1.3.17, from Alcaligenes Sp. Lyophilized powder, 13 Units/mg) and acetylcholine (ACh) were purchased from Sigma-Aldrich. Mercaptopropionic acid (MPA) was obtained from Alfa Aesar. Tellurium powder, cadmium nitrate, sodium borohydride were purchased from Institute of Tianjin Jinke Fine Chemicals. The standard sample of dichlorvos (1.00 mg/mL in Methanol) was purchased from National Institute of Metrology. The reagents such as cadmium nitrate and sodium borohydride were of analytical grade and used without further purification. Phosphate Buffer (PB) was prepared: 189.4 mM Na_2HPO_4, 10.6 mM NaH_2PO_4, pH 8.0. The ultrapure water (0.22 μm) was produced using a Millipore-Q water system.

The UV–vis absorption spectra were measured using Jasco V-570 UV–vis spectometer. The fluorescence measurements were recorded with a Cary Eclipse fluorescence spectrophotometer (Varian, Inc.). The sample was excited at 400 nm, and emission spectra were recorded in the wavelength of 520–680 nm. The exciting slit and the emission slit were both 5 nm. The samples for the fluorescence measurements were placed in a 10 mm optical path length quartz fluorescence cuvette.

2.2. Synthesis of water-soluble CdTe QDs

The CdTe QDs were synthesized in the aqueous phase according to the reported method with minor modification (Gaponik et al., 2002). Briefly, freshly prepared NaHTe solution was added to nitrogen-saturated $Cd(NO_3)_2$ solutions at pH 11.2 (adjusted by dropwise addition of 1 M NaOH) in the presence of mercaptopropionic acid (MPA) as stabilizing agent. Then the CdTe precursor solution was heated in 95 °C water bath. The precursor concentrations were $[Cd^{2+}]=10$ mM, [MPA]=24 mM, and $[Te^{2-}]=5$ mM.

As shown in Fig. S1(a), a series of QDs with maximum emission wavelength ranging from 535 nm to 630 nm were obtained with the reaction time prolonged. When the reaction time was 13 h, the fluorescence intensity at the maximum emission wavelength (600 nm) reached a maximum with the same concentration. As a result, in this work we used QDs with a maximum emission wavelength of 600 nm. According to Fig. S1(b), the wavelength of the first excitonic absorption peak is 558 nm, so the size of QDs is

3.32 nm, and the concentration of the QDs was 2×10^{-5} M (Yu et al., 2003).

2.3. Detection of DDVP in phosphate buffer

The procedure for DDVP determination was as follows: (1) AChE was first incubated with Phosphate Buffer (pH=8.0) containing different concentrations of DDVP at certain temperature for a period of time; (2) ChO*x*, QDs and ACh were stepwise added in the above solution and the fluorescence signal was monitored over time.

2.4. Measurement and calibration of DDVP residues in apples

DDVP determination procedure in real apple samples was described as follows: (1) the apple was first chopped and extracted with 20 mL Phosphate Buffer (pH=8.0) (Zheng et al., 2011a; Zheng et al., 2011b); (2) AChE was incubated with the extracted solution at 37 °C for 15 min; (3)ChO*x*, QDs and ACh were stepwise added in the above solution and the fluorescence signal was monitored over time. The results were compared with the calibration curve, and the DDVP concentration could be obtained.

3. Results and discussion

3.1. Principle of CdTe QDs fluorescence switch

Scheme 1(a) illustrates the fluorescence switch mechanism for the detection of DDVP based on CdTe QDs, which are synthesized in the aqueous phase. It is found that H_2O_2 can efficiently decrease the fluorescence intensity of QDs (Mancini et al., 2008). The ACh decomposes to choline and acetric acid through the AChE catalyzed reaction, then the choline can be decomposed to betaine and H_2O_2 by ChO*x* catalyzing. Along with the consecutive enzyme reactions, the fluorescence intensity of QDs decreases gradually.

Fig. 1(a) shows a typical time-dependent fluorescence intensity of 0.2 μM QDs that are mixed with 125 U/L ChO*x*, 250 U/L AChE and 500 μM ACh. As the time is prolonged, the fluorescence intensity decreases, accompanied with a blue shift of the peak maxima. That is believed to originate from preferential PL quenching of CdTe QDs with large sizes, because of the close energy levels between valence bands of large CdTe QDs and the oxidation potential of H_2O_2 (Andreescu and Marty, 2006; Masumoto and Sonobe, 1997; Reiss et al., 2009).

We define K_t as the retained percentage of fluorescence intensity ($K_t=F_t/F_0$), where F_0 and F_t are the absolute fluorescence intensity values recorded at 600 nm before and after addition of acetylcholine, respectively.

When it is introduced in solution, DDVP can bind selectively to the active centers of AChE, which causes a reduction in the rate of AChE catalyzed reaction. Thus, the rate of hydrogen peroxide formation decreases, which leads to the decrease of the fluorescence quenching rate. As an example, Fig. 1(b) shows the change of K_t with different concentration of DDVP (0.45 μM, 3.37 μM, 6.78 μM) and K_t without DDVP with time in the presence of 250 U/L ChO*x*, 500 U/L AChE and 500 μM ACh. It can be seen that the K_t value change over time appears to approximate an exponential decay curve. When DDVP (0.45 μM, 3.37 μM, and 6.78 μM) is added, the decrease rate of K_t is inversely proportional to DDVP concentration. Accordingly, the fluorescence intensity increases with the increase of the concentration of DDVP. In other words, when there was more DDVP in the sample, more AChE was inhibited by DDVP. As a result, the amount of H_2O_2 produced from the enzyme reaction decreased, which was followed by the decrease of the quenching degree for QDS.

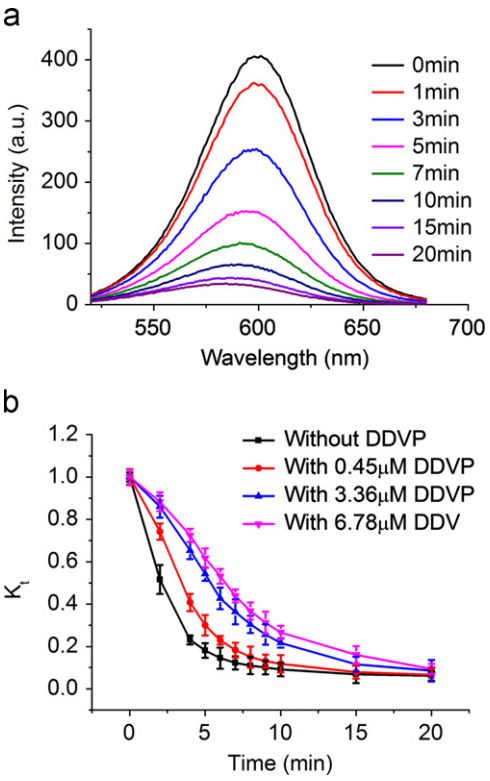

Fig. 1. (a) Typical time-dependent fluorescence intensity of 0.2 μM QDs in the presence of 125 U/L ChO*x*, 250 U/L AChE and 500 μM Ach; (b) the quenching kinetic of fluorescence intensity without DDVP and with different concentrations of DDVP (0.45 μM, 3.37 μM, 6.78 μM). Error bars in Fig. 1(b) represent the standard deviations of three independent measurements.

3.2. Optimization of the experimental conditions

The sensitivity of the proposed biosensor is related to many factors, such as the pH of the solution, the concentration of enzyme, the temperature and time for the incubation of DDVP and AChE, so the experimental conditions are optimized for determination of concentration of DDVP. The optimum pH values of AChE and ChO*x* are pH 8.0–9.0 and 7.0–8.0, respectively (Gao et al., 2012). As a result, all the following experiments were carried out in the pH 8.0 PB solution. Furthermore, all the following experiments were performed in the presence of 4.5 μM DDVP, 0.2 μM QDs and 500 μM Ach, which presented in an excess amount.

We use Influence Coefficient of OPs (I_t) as a signal for the detection of OP compounds.

$I_t=K_{t\ with\ DDVP}/K_{t\ without\ DDVP}$, where $K_{t\ with\ DDVP}$ is the retained percentage of fluorescence intensity (K_t) with different concentrations of DDVP and $K_{t\ without\ DDVP}$ is the retained percentage of fluorescence intensity (K_t) without DDVP. (See Fig. 1(b)).

We first investigated the influence of the enzyme concentration on I_t values (Fig. 2(a)). The AChE concentrations adopted in this study were 0.25, 0.5, and 0.75 U/ml. The incubating time and temperature were constant. The results clearly indicated that the optimum concentration of AChE required for effective Influence Coefficient of OPs was 0.5 U/ml. It was observed that, if AChE concentration was decreased below or increased above 0.5 U/ml, there was significant decrease in I_t values. It can be seen that in Fig. 2(a), the maximum I_t value of 3.26 is obtained using 0.5 U/ml AChE concentration.

Furthermore, the incubating temperature of AChE and DDVP were optimized. The temperature adopted in this study were 25 °C and 37 °C. The AChE concentration of 0.5 U/ml and constant

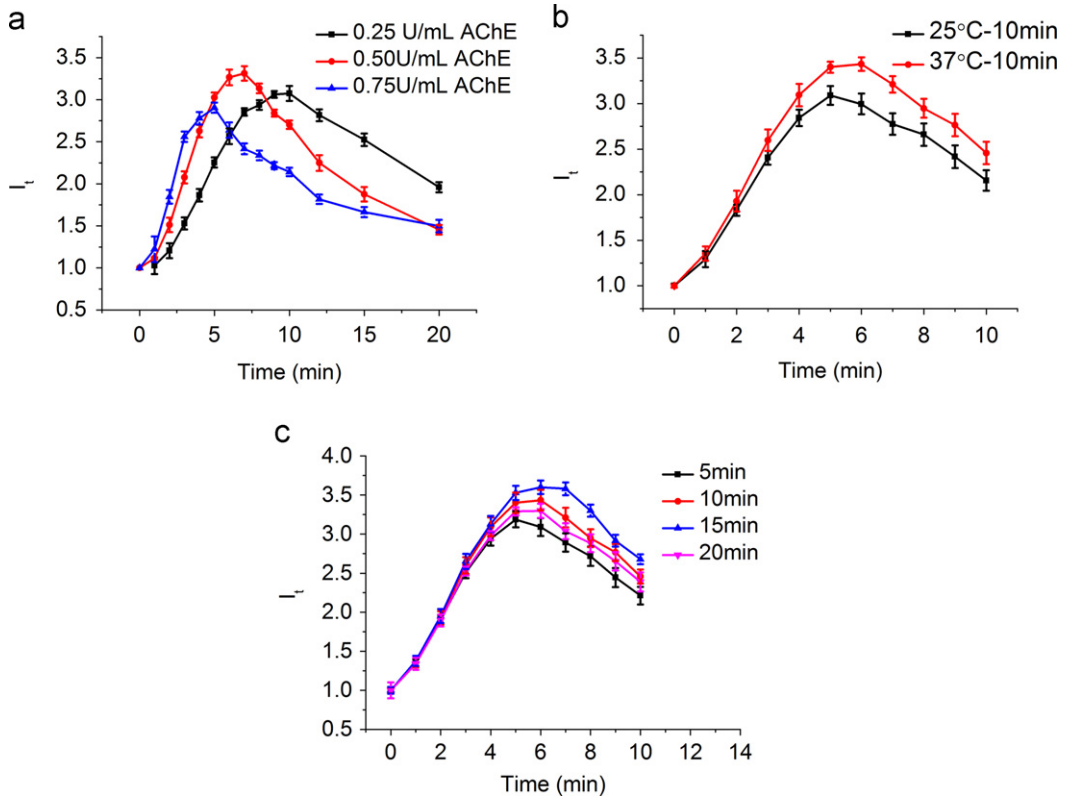

Fig. 2. Influence coefficient of OPs (I_t) at 600 nm as a function of (a) the concentration of enzyme; (b) the incubating temperature of AChE and DDVP; (c) the incubating time of AChE and DDVP. Error bars represent the standard deviations of three independent measurements.

incubating time were used. The variation in the incubating temperature versus I_t values is shown in Fig. 2(b).The results clearly indicated that the maximum I_t value was obtained at 37 °C when the time is 6 min.

Lastly, we investigated the influence of the incubating time on Influence Coefficient of OPs. In order to optimize the incubating time, different incubating times selected for the study were 5, 10, 15, and 20 min. The AChE concentration of 0.5 U/ml and incubating temperature of 37 °C were maintained constant. It could be seen that the I_t value increased gradually up to a maximum value with the increasing of incubating time to 15 min, followed by a decrease for further increasing the incubating time. The maximum I_t value was obtained at 15 min as shown in Fig. 2(c).

In summary, the optimum experimental conditions are as follows: 250 U/L ChO*x*, 500 U/L AChE and 500 μM ACh, AChE reacted with DDVP at 37 °C for 15 min.

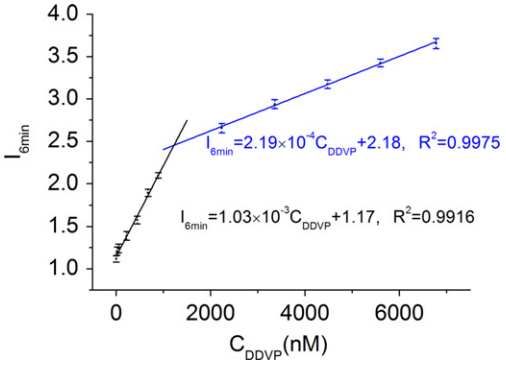

Fig. 3. The plot of influence coefficient of OPs vs. DDVP concentration of the proposed biosensor. Error bars represent the standard deviations of five independent measurements.

3.3. Detection of DDVP in phosphate buffer

Under the optimum experimental conditions established in the above studies, calibration plots were generated for DDVP (Fig. 3). The results exhibited a good linear relationship in the range of 4.49–896 nM and 2240–6780 nM with different slopes, and the slope of low concentration (4.49–896 nM) was bigger than that of the high concentration (2240–6780 nM). Such situation was also observed by several other groups (Chen et al., (2011); Zhang et al., 2010)).

The proposed method shows good sensitivity for the detection of DDVP. The LOD of 4.49 nM (~1 μg/L) for dichlorvos is 500 times lower than that of AChE biosensors (Dondoi et al., 2006), the same order of magnitude with that of the GC/MC method (1 μg/L) (Amendola et al., 2002) and that from the three-electrode biosensor (R-DmAChE, MWCNTs and Prussian blue) (0.5 μg/L) (Tang et al., 2011). Thus, the sensitivity of the proposed method is acceptable. According to the EC 149-2008 (Residue Standard of the European Union), the detectable pesticide concentration in imported fruits and vegetables should be lower than 100 μg/L (0.45 μM) for dichlorvos. The LOD of the proposed method is enough to satisfy current detection requirement. Scheme 1(c) shows the corresponding fluorescence picture of QDS excited at 254 nm with different concentrations of DDVP (Without DDVP, 0.45 μM DDVP, 6.78 μM DDVP) and it could be distinguished with the naked eye. Hence the proposed methods in this paper achieve a multidimensional sensing of DDVP.

3.4. The anti-interference ability and reproducibility

The interference study is one of the most important evaluations of the biosensor. Fig. S2(a) shows the I_{6min} of 4.48 μM DDVP (see "D" in Fig. S2(a)). Then the additions of 10 mM lactic acid (see "D+LA" in Fig. S2(a)), 100 μM ascorbic acid (see "D+AA" in Fig. S2(a)),

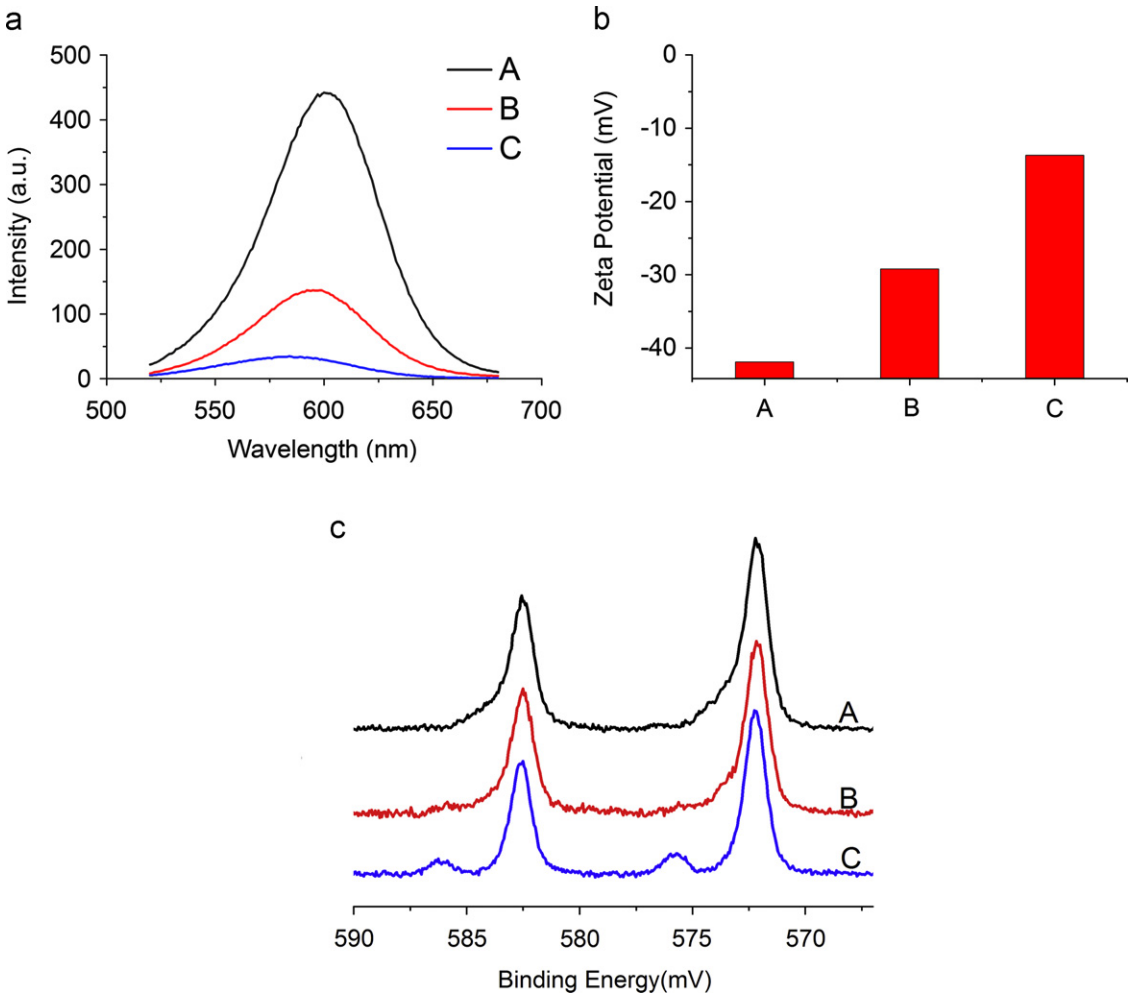

Fig. 4. (a) The fluorescence intensity of 0.2 μM QDs with different quenching degree; (b) zeta potential of water-soluble CdTe QDs with different quenching degrees; (c) photoemission spectra of Te(3d) levels of QDs with different quenching degrees. A, pristine QDs; B, QDs quenched by 1 mM H_2O_2; C, QDs quenched by 4 mM H_2O_2.

15 mM KCl (see "D+KCl" in Fig. S2(a)), and 15 mM sodium citrate (see "D+SC" in Fig. S2(a)) did not cause any observable changes in the I_{6min} of the system. The results proved that the proposed biosensor can provide credible anti-interference ability.

In addition, the reproducibility of the biosensor fabrication procedure was evaluated by comparing the different days response of the determination of 2.24 μM DDVP (see Fig. S2(b)). The relative standard deviation (RSD) was 2.24% for 6 assays with an average response of 2.61.

3.5. Study the quenching mechanism of enzyme reaction on the fluorescence of QDs

The control experiment of DDVP detection (Fig. S3) showed that there was no significant interference on the fluorescence of QDs observable from the 15 μM DDVP, which is higher than the range of detection (4.49–6780 nM). Furthermore, it was also proven that no observable interference on the fluorescence of QDs was observed in the presence of AChE, ChO*x* and ACh (Chen et al., (2011)). All these results proved that the formation of H_2O_2 (shown in Scheme 1(a)) is essential to quench the emission maximum of the QDs.

In terms of the quenching mechanism of H_2O_2 on the fluorescence of QDs, there are two possible courses. Some papers assume that the MPA tagged on the surface of the QDs through Cd–S bonding are detached from the surface of QDs and oxidized to form a disulfide product (RS–SR) in the presence of H_2O_2 (Dasog and Scott, 2007; Shiang et al., 2009). Others put forward an alternative explanation of the quenching of QDs, stating that the quenching mechanism of QDs was the oxidation of tellurium in QDs (Chen et al., (2012)).

Herein, it is observed that both of the explanations are involved in the quenching of QDs. The detaching of MPA is accompanied with the decrease of –COOH on the surface of QDs, which will lead to the increase of the Zeta potential of QDs during the process. We tested the Zeta potential of QDs with different quenching degree, whose fluorescence emission spectra are shown in Fig. 4 (a). The pristine QDs show well fluorescence intensity at 600 nm. By quenching the QDs with 1 mM H_2O_2, the fluorescence intensity decreases by 69%. When the concentration of H_2O_2 is increased to 4 mM, the fluorescence intensity decreases by 93.4%. The change of the Zeta potential of the different QDs can be seen from Fig. 4(b). The successive increase of the Zeta potential is obviously observed during the QDs quenching process, which is result of the increase of MPA detaching from the QDs surface.

X-ray photoemission spectroscopy (XPS) stands out as a useful tool for investigating the local binding properties in materials science. In this way, a characterization of the chemical environment of QDs specific atoms can be given. Fig. 4(c) is the characteristic XPS region spectra (Te $3d_{5/2}$ and Te $3d_{3/2}$ peaks) for QDs with different quenching degrees (see Fig. 4(a)). The Te $3d_{5/2}$ peak at a binding energy of 572.4 eV corresponds to Te–Cd bonds, and the Te $3d_{5/2}$ peak at a binding energy of 575.6 eV corresponds to Te–O bonds. When the QDs are quenched by 4 mM H_2O_2, the

Table 1
Recovery ratios of DDVP in fruit samples.

Sample	I_{6min}	Results of experiment (μM)	RSD (%)	Actual amount (μM)	Recovery (%)
Apple	1.04 ± 0.04				
Apple with DDVP	1.95 ± 0.01	0.76 ± 0.01	1.34	0.78	97.07
Apple with DDVP	2.87 ± 0.02	3.14 ± 0.11	3.48	3.12	100.87

oxidation of Te can be observed. What is more, the relative atomic percentage of S_{2p} can be calculated from the XPS results. The relative atomic percentages of S_{2p} for QDs with different quenching degrees are 9.25%, 8.89% and 8.16%, which decreases with the increase of quenching degree. The result demonstrates the change of the amount of MPA tagged on the surface of the QDs can track the progress of quenching.

In summary, the coincidence of the detaching of MPA and the oxidation of Te is observed during the QDs quenching. At the initial stage of the quenching of QDs, the reason for the quenching was mainly the detaching of thiolation from the surface of QDs. After that, the quenching of QDs was due to the combination of thiolation detaching and oxidation of Te.

3.6. Determination of DDVP content in fruit samples

Sample pretreatment is a complex multiple-step procedure for pesticide determination in real samples for chromatography methods. The pesticide needs to be extracted by organic media and concentrated afterwards, which are time-and cost-consuming and are prone to pesticide loss. Liu et al. proposed a new method for fruits pretreatment without using organic solvents and tedious preconcentration steps (Zheng et al., 2011a; Zheng et al., 2011b). Using this method, the apple was first chopped and extracted with 20 mL Phosphate Buffer (pH=8.0). The apple with a low I_t (1.04 ± 0.04) was used as reference sample. Further experiments were carried out with the intentional addition of dichlorvos. We found that the recovery of DDVP is almost 100%. As a result, the proposed method has good performance in detection of dichlorvos in fruit samples.

4. Conclusions

In this paper, a novel biosensor in liquid phase was constructed based on inhibition mechanism of AChE. The biosensor was composed of enzyme (AChE and ChO*x*), QDs and substrate (ACh), without any complex process of assembly for biosensor. With the developed biosensor we successfully detected organophosphorus pesticides in real samples. What is more, a possible mechanism is put forward to explain the fluorescence quenching of CdTe QDs in the presence of H_2O_2. The quenching of QDs is due to the coincidence of the detaching of MPA and the oxidation of Te. The proposed biosensor offers many advantages, such as easy sample treatment, simple process of detection, high sensitivity and low cost. By a combination with automatic biochemistry analyzer, the biosensor will be possible to develop a method for rapid high-throughput detection of organophosphorus pesticide residues. Table 1

Acknowledgments

We acknowledge financial support from the National Natural Science Foundation of China (Project no. 81171454, 61171049, and 61178035).

Appendix A. Supporting information

Supplementary data associated with this article can be found in the online version at http://dx.doi.org/10.1016/j.bios.2013.03.053.

References

Amendola, L., Botrè, F., Carollo, A.S., Longo, D., Zoccolillo, L., 2002. Analytica Chimica Acta 461, 97–108.
Andreescu, S., Marty, J.L., 2006. Biomolecular Engineering 23, 1–15.
Chen, Z., Ren, X., Meng, X., Chen, D., Yan, C., Ren, J., Yuan, Y., Tang, F., 2011. Biosensors and Bioelectronics 28, 50–55.
Chen, Z., Ren, X., Meng, X., Zhang, Y., Chen, D., Tang, F., 2012. Analytical Chemistry 84, 4077–4082.
Constantine, C.A., Gattás-Asfura, K.M., Mello, S.V., Crespo, G., Rastogi, V., Cheng, T.C., DeFrank, J.J., Leblanc, R.M., 2003. Journal of Physical Chemistry B 107, 13762–13764.
Curl, C.L., Fenske, A.R., Kissel, C.J., Shirai, H.J., Moate, F.T., Griffith, W., Coronado, G., Thompson, B., 2002. Environmental Health Perspectives 110, 787–792.
Dasog, M., Scott, R.W.J., 2007. Langmuir 23, 3381–3387.
Dondoi, M.P., Bucur, B., Danet, A.F., Toader, C.N., Barthelmebs, L., Marty, J.L., 2006. Analytica Chimica Acta 578, 162–169.
Gao, X., Tang, G., Su, X., 2012. Biosensors and Bioelectronics 36, 75–80.
Gaponik, N., Talapin, D.V., Rogach, A.L., Hoppe, K., Shevchenko, E.V., Kornowski, A., Eychmüller, A., Weller, H., 2002. Journal of Physical Chemistry B 106, 7177–7185.
Hossain, S.M., Luckham, R.E., McFadden, M.J., Brennan, J.D., 2009. Analytical Chemistry 81, 9055–9064.
Karnati, C., Du, H., Ji, H.F., Xu, X., Lvov, Y., Mulchandani, A., Mulchandani, P., Chen, W., 2007. Biosensors and Bioelectronics 22, 2636–2642.
Mancini, M.C., Kairdolf, B.A., Smith, A.M., Nie, S., 2008. Journal of American Chemical Society 130, 10836–10837.
Masumoto, Y., Sonobe, K., 1997. Physical Review B 56, 9734–9737.
Reiss, P., Protière, M., Li, L., 2009. Small 5, 154–168.
Sarabia, L., Maurer, I., Bustos-Obregon, E., 2009. Ecotoxicology and Environmental Safety 72, 663–668.
Shenouda, J., Green, P., Sultatos, L., 2009. Toxicology and Applied Pharmacology 241, 135–142.
Shiang, Y.C., Huang, C.C., Chang, H.T., 2009. Chemical Communications 23, 3437–3439.
Sotiropoulou, S., Fournier, D., Chaniotakis, N.A., 2005. Biosensors and Bioelectronics 20, 2347–2352.
Su, S., He, Y., Zhang, M., Yang, K., Song, S., Zhang, X., Fan, C., Lee, S.T., 2008. Applied Physics Letters 93, 023113.
Sunkaria, A., Wani, W.Y., Sharma, D.R., Gill, K.D., 2012. Chemical Research in Toxicology 25, 1762–1770.
Suwansa-ard, S., Kanatharana, P., Asawatreratanakul, P., Limsakul, C., Wongkittisuksa, B., Thavarungkul, P., 2005. Biosensors and Bioelectronics 21, 445–454.
Tang, Z., Chen, H., Song, S., Fan, C., Zhang, D., Wu, A., 2011. Journal of AOAC International 94, 307–312.
Vamvakaki, V., Chaniotakis, N.A., 2007. Biosensors and Bioelectronics 22, 2848–2853.
Yadav, P., Jadhav, S., Kumar, V., Kaul, K., Pant, S., Flora, S., 2012. Interdisciplinary Toxicology 5, 1–8.
Yu, W.W., Qu, L., Guo, W., Peng, X., 2003. Chemistry of Materials 15, 2854–2860.
Zhang, K., Mei, Q., Guan, G., Liu, B., Wang, S., Zhang, Z., 2010. Analytical Chemistry 82, 9579–9586.
Zheng, Z., Li, X., Dai, Z., Liu, S., Tang, Z., 2011a. Journal of Materials Chemistry 21, 16955.
Zheng, Z., Zhou, Y., Li, X., Liu, S., Tang, Z., 2011b. Biosensors and Bioelectronics 26, 3081–3085.